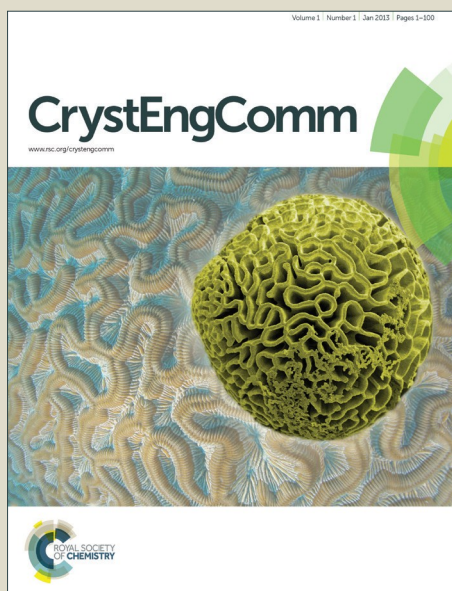


CrystEngComm

Accepted Manuscript



This article can be cited before page numbers have been issued, to do this please use: F. Vita, M. Vorti, G. Orlandini, V. Zanichelli, C. Massera, F. Ugozzoli, A. Arduini and A. Secchi, *CrystEngComm*, 2016, DOI: 10.1039/C6CE00268D.



This is an *Accepted Manuscript*, which has been through the Royal Society of Chemistry peer review process and has been accepted for publication.

Accepted Manuscripts are published online shortly after acceptance, before technical editing, formatting and proof reading. Using this free service, authors can make their results available to the community, in citable form, before we publish the edited article. We will replace this *Accepted Manuscript* with the edited and formatted *Advance Article* as soon as it is available.

You can find more information about *Accepted Manuscripts* in the [Information for Authors](#).

Please note that technical editing may introduce minor changes to the text and/or graphics, which may alter content. The journal's standard [Terms & Conditions](#) and the [Ethical guidelines](#) still apply. In no event shall the Royal Society of Chemistry be held responsible for any errors or omissions in this *Accepted Manuscript* or any consequences arising from the use of any information it contains.



Journal Name

ARTICLE

Synthesis and Recognition Properties of Calix[4]arene Semitubes as Ditopic Hosts for *N*-alkyl-pyridinium Ion Pairs

Francesco Vita, Michela Vorti, Guido Orlandini, Valeria Zanichelli, Chiara Massera, Franco Uguzzoli,* Arturo Arduini, and Andrea Secchi*

Received 00th January 20xx,
Accepted 00th January 20xx

DOI: 10.1039/x0xx00000x

www.rsc.org/

A series of calix[4]arene semitubes (**4a-c**) having alkyl bridging spacers of different length and flexibility on their lower rim was synthesised and characterised in solution and in the solid state by ^1H NMR spectroscopy and X-ray crystallography. The binding properties of these novel ditopic hosts toward a series of *N*-alkyl pyridinium ion pairs were investigated in low polar media by ^1H NMR and UV-Vis spectroscopy and compared with those of the corresponding calix[4]arene monotopic host **5**. These studies showed that in low polar solvents the calix[4]arene semitubes behave as homoditopic hosts giving rise with *N*-alkyl pyridinium ion pairs to supramolecular adducts of 1:2 host-guest stoichiometry.

Introduction

Molecular self-assembly is a process in which molecules spontaneously form, through non-covalent interactions, ordered aggregates whose structure, in equilibrium conditions, is determined by the chemical information present in the components of the assembly.^{1,2} The clever exploitation of self-assembly can in principle give access to a range of complex supramolecular entities endowed with specific physical and chemical properties which otherwise would be considered impossible to construct.³ Enticing examples of these type are represented by supramolecular polymers (SP), which are ensembles of suitable monomer units held together by reversible non-covalent intermolecular interactions.⁴⁻⁷ These assemblies are frequently composed of two or more components endowed with complementary structural features and chemical information. They are attracting an increasing attention by the scientific community because they combine part of the properties of conventional polymers with those conferred by the weak and reversible interactions among its components.⁸⁻¹⁰

Within the plethora of synthetic macrocyclic compounds employed for the preparation of SP,¹¹⁻¹³ the use of calixarene-based hosts¹⁴ is increasing over the years.¹⁵⁻²² These compounds are indeed characterised by a π -rich aromatic cavity that, if properly functionalised and rigidified, can be exploited for self-assembly processes through the recognition of neutral or charged species.¹⁴ We have recently verified that both calix[6]arene and calix[4]arene-based hosts having *N*-phenylurea groups at their larger (upper) rim may interact with ditopic guests based on *N,N'*-dialkyl-4,4'-bipyridinium

(viologen) ion pairs giving rise to 2:1 host-guest self-assembled capsules in solution of low polar solvents^{23,24} and in the solid state.²⁵ Viologen-based guests are endowed with interesting redox properties,²⁶ and it has been already shown as their affinity for the calixarene cavity²⁷⁻³¹ can be turned on and off depending on their oxidation state.²⁷ Supramolecular adducts of this type can thus represent the prototype for the development of novel guest-driven supramolecular polymers and stimuli-responsive materials.³²⁻³⁷ The pursuing of this aim, however, necessarily implies the design of suitable ditopic hosts capable of linking difunctional guests in a linear structural motif.³⁸⁻⁴⁰ Herein we report on the synthesis of a series of novel ditopic calix[4]arene-based hosts and their complexation properties in solution of weakly polar media towards a series of *N*-alkyl pyridinium ion pairs as the guests.

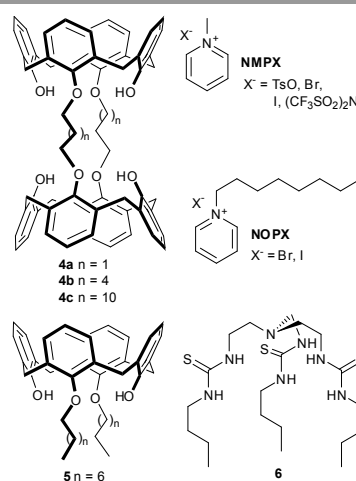


Chart 1. Calix[4]arene-based ditopic (**4a-c**) and monotopic (**5**) hosts; *N*-alkyl pyridinium (NMPX and NOPX) guests; and the anion host **6** employed in this study.

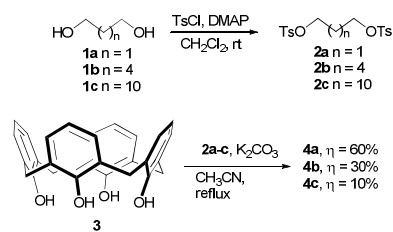
Dipartimento di Chimica, Università degli Studi di Parma, Parco Area delle Scienze 17/A, I-43124 Parma, Italy.

Results and discussion

Synthesis of the ditopic hosts.

The design of the ditopic hosts was based on the analysis of the literature,^{41–44} which showed that the bridging of two calix[4]arene macrocycles through their lower rim with two alkyl spacers, would result in so-called calix[4]arene "semitubes",⁴⁵ whose binding sites, i.e. the two π -rich aromatic cavities, have the proper geometrical arrangement to yield SP. In particular, we tackled the synthesis of a series of novel calix[4]arenes semitubes having bridging units of three (**4a**), six (**4b**) and twelve (**4c**) methylene groups, respectively (see Chart 1). We chose to study alkyl spacers of different length in order to evaluate how the bridge flexibility and the distance between the two aromatic cavities may affect the recognition of two positively charged guests. The use of doubly bridged bis-calix[4]arene host systems rather than the tetra-bridged ones⁴⁶ was prompted by the following considerations: *i*) lower rim partially alkylated calix[4]arene hosts have a highly pre-organised π -donor cavity suitable for the recognition of charged²⁵ and small neutral^{47–50} organic species in weakly polar solvents, and *ii*) the free phenolic groups may promote ion-pairs recognition by acting as hydrogen-bond donor binding sites.

In a one-pot reaction, calix[4]arene **3** was reacted in refluxing acetonitrile in the presence of K_2CO_3 and the appropriate ditosylate linker (**2a–c**), using a 1:2:2 stoichiometric ratio between the reagents (see Scheme 1). In these conditions, the "short" calix[4]arene semitube **4a** was recovered in 60% yield, while the more flexible hosts **4b** and **4c** were isolated in 20 and 10% yield, respectively, after chromatography separation. All hosts were characterised through NMR spectroscopy, elemental analysis and mass spectrometry. Unlike **4b** and **4c**, the 1H NMR spectroscopic characterisation of **4a** in solution was accomplished in CD_2Cl_2 because of its poor solubility in chloroform. The 1H -NMR spectrum of **4a** recorded at 300 MHz is depicted in Fig. 1, and it shows a singlet at $\delta = 8.89$ ppm, which was assigned to the 4 equivalent phenolic protons of the macrocycles lower rims.



Scheme 1. Synthesis of calix[4]arene semitubes **4a–c**.

The pattern of the aromatic signals, the two overlapped doublets at ca. 7.1 ppm, integrating for 16 protons, and two well-separated triplets at $\delta = 6.89$ and 6.64 ppm, each integrating for 4 protons, is consistent with calix[4]arene macrocycles adopting a flattened *cone* conformation on the NMR time-scale. As expected, considering the symmetry of this bis-calix[4]arene host, the bridging methylene groups give rise to a typical AX system of two doublets with geminal coupling of 13 Hz at $\delta = 4.46$ and 3.48 ppm. The two propyl chains, linking head-to-head the calix[4]arene macrocycles, are responsible for a multiplet integrating for 8 protons at ca. 4.4 ppm and a quintuplet integrating for 4 protons at $\delta = 3.17$ ppm. Besides the signals arising from their longer C6 and C12 linking alkyl chains, the 1H -NMR spectra of **4b** and **4c**, taken in $CDCl_3$, show a NMR signals pattern very similar to that of **4a** (see Fig. 3g).

Solid state studies. Crystals suitable for the X-rays structure analysis of calix[4]arenes **4a** and **4b** were obtained from the slow evaporation of their solution in dichloromethane and chloroform, respectively. **4a** crystallizes with two symmetry-independent molecules in the unit cell. The two molecules (see Fig. 2a), although slightly different from each other in size and conformation, are both centrosymmetric and the conformation of their calix[4]arene baskets are blocked by intramolecular O-H...O hydrogen bonds between phenolic OH groups (see Table 1 for the geometrical parameters).

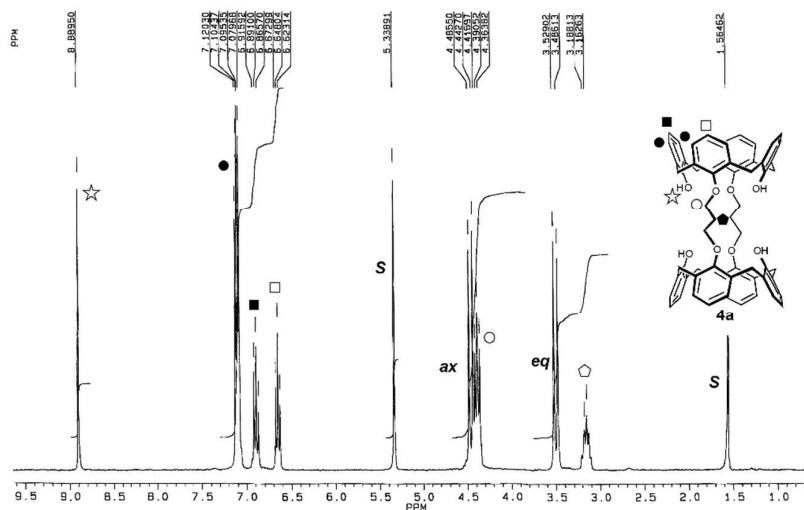


Fig. 1. $^1\text{H-NMR}$ (300 MHz) of calix[4]arene semitube **4a** in CD_2Cl_2 (resonances assignment has been indicated with symbols on the calix[4]arene sketch).

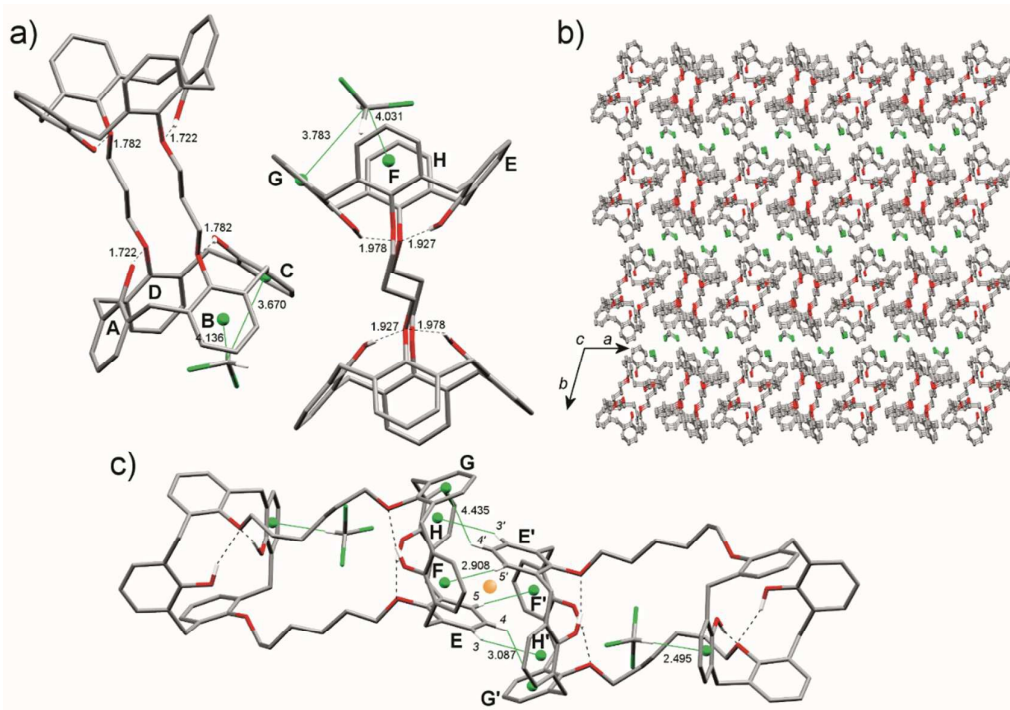


Fig. 2. a) Stick view of the X-ray structure of the two independent molecules present in the unit cell of calix[4]arene semitube **4a** and b) ball and stick view of their self-assembly in the crystal lattice. Only the relevant hydrogen atoms are reported for clarity, while the intramolecular hydrogen bonds and CH/π interactions were highlighted with black dashed and continuous green lines, respectively; c) stick view of the self-assembly of the mutual inclusion motif between adjacent calix[4]arenes sub-units in calix[4]arene semitube **4b** in the crystal lattice (colours: C grey, O red, Cl green H white; centroids of benzene rings, green.; centre of symmetry, orange).

In the **ABCD** macrocycle (and in its centrosymmetric one) the calix[4]arene is blocked in a “flattened” cone conformation by the two hydrogen bonds $\text{O1A-H}\cdots\text{O1D}$ and $\text{O1C-H}\cdots\text{O1B}$, whereas in the **EFGH** macrocycle (and in its centrosymmetric one) the phenolic oxygen O1H accepts contemporarily the two hydrogen bonds donated by the OH groups at the phenolic rings E and G. In both macrocycles, a CH_2Cl_2 molecule is anchored to two adjacent benzene rings through attractive CH/π interactions.^{51,52} All the $\text{C}(\text{CH}_2\text{Cl}_2)\cdots\text{Centroid}(\text{CT})$ separations ($\text{C}\cdots\text{CT-B}$ 4.136 Å, $\text{C}\cdots\text{CT-C}$ 3.670 Å e $\text{C}\cdots\text{CT-G}$ 3.738 Å, $\text{C}\cdots\text{CT-H}$ 4.031 Å) lie in the range where the binding energy between benzene and dichloromethane is attractive.⁵³ In the crystal lattice, **4a** and CH_2Cl_2 self-assemble giving rise to layers of CH_2Cl_2 molecules intercalated between layers of calix[4]arene semitubes parallel to the crystallographic ac plane (Fig. 2b).

Table 1. Geometrical parameters for intramolecular hydrogen bonds in calix[4]arene semitubes **4a** and **4b** (D and A denote donor and acceptor atoms, respectively)

	H-bonds	D...A (Å)	H...A (Å)	D-H...A (°)
4a	$\text{O1B-H}\cdots\text{O1A}$	2.755	1.823	169.8
	$\text{O1D-H}\cdots\text{O1A}$	2.909	1.982	167.5
	$\text{O1F-H}\cdots\text{O1E}$	2.765	1.898	159.3
	$\text{O1H-H}\cdots\text{O1G}$	2.689	1.834	158
4b	$\text{O1A-H}\cdots\text{O1D}$	2.727	1.782	155.9
	$\text{O1C-H}\cdots\text{O1B}$	2.707	1.722	162.2
	$\text{O1E-H}\cdots\text{O1H}$	2.852	1.978	144.5
	$\text{O1G-H}\cdots\text{O1H}$	2.893	1.927	164.86

In the molecular structure of **4b** (see Fig. 2c), the two calix[4]arene sub-units are still blocked in the flattened cone conformation by four strong intramolecular hydrogen bonds: the phenolic oxygen O1A in the **ABCD** macrocycle acts as “bifurcated” acceptor of the two hydrogen bonds $\text{O1B-H}\cdots\text{O1A}$ and $\text{O1D-H}\cdots\text{O1A}$, whereas the two simple $\text{O1F-H}\cdots\text{O1E}$ and $\text{O1H-H}\cdots\text{O1G}$ hydrogen bonds block the mutual orientations on the phenolic rings in the **EFGH** calix[4]arene (see Table 1). One chloroform solvent molecule is linked *via* strong CH/π interactions to the aromatic ring A. The geometrical parameters of the CH/π interactions, $\text{C}\cdots\text{CT}$ 3.392 Å, $\text{H}\cdots\text{CT}$ 2.495 Å, $\text{C-H}\cdots\text{CT}$ 155.8°, are almost identical to the values found by Tsuzuki et al.,⁵⁴ in the high level ab-initio quantum chemical calculations of the intermolecular interactions in the benzene- CHCl_3 complex.

A second chloroform molecule fills the voids of the crystal lattice. More interesting is the self-assembly of calixarenes and CHCl₃ solvent molecules in **4b**: two adjacent calix[4]arene are mutually included one into another giving rise to the centrosymmetric dimers shown in Fig. 2c. The structure-directing factor which leads to the self-assembly in centrosymmetric dimers is the network of the six CH/π interactions evidenced in Fig. 2c with green lines. Contrary to **4a**, in the X-ray crystal structure of **4b** a CHCl₃ molecule is bound outside the cavity thus favouring, probably as consequence of the larger flexibility of the longer alkyl bridging chains, the self-assembly of two calix[4]arene subunits.

Table 2. Geometrical parameters for CH/π interactions in calix[4]arene semitube **4b**.^a

C-H...CT	H...CT (Å)	C...CT (Å)	C-H...CT (°)
C3E-H...CTH'	3.087(6)	3.942(7)	149.0(4)
C4E-H...CTG'	3.058(7)	3.761(7)	131.3(4)
C5E-H...CTF'	2.908(6)	3.810(7)	157.1(5)

^a CT indicates the centroid of the aromatic rings; the three H atoms of the phenolic ring E act as donor groups to the three aromatic rings of the phenolic rings F' G' H' of the centrosymmetric calixarene unit and contemporarily the three H atoms of the phenolic ring E' act as donor groups to the three aromatic rings of the phenolic rings F G H.

The unexpected different complexing mode experienced by **4a** and **4b** suggests a possible different behaviour as ditopic hosts also for organic ion pairs. This prompted us to investigate the binding abilities of **4a-c** towards the series of *N*-methyl pyridinium salts (NMPX) illustrated in Chart 1. It is indeed known that the electron-poor NMP cation can efficiently interact with the π-rich aromatic cavity of preorganised rigid monotopic calix[4]arene hosts, giving rise to inclusion complexes in the solid state.^{23,55} Unfortunately, the several attempts so far accomplished to crystallise the inclusion complex between these pyridinium salts and **4a-c**, from the corresponding 2:1 mixtures in dichloromethane, failed. Therefore, the binding properties of these ditopic hosts have been evaluated in weakly polar solvents through NMR and UV-vis spectroscopies.

NMR binding studies. The binding properties of calix[4]arene semitubes **4a-c** were preliminary evaluated toward a series *N*-alkyl pyridinium salts (NMPX and NOPX, see Chart 1) characterised by: a) anions of different coordination strength (from the lowest to the highest X = (CF₃SO₂)₂N, I, Br, and TsO) and b) different bulkiness of the alkyl substituent on the iminium nitrogen. This choice was based considering that in weakly polar solvents these species are present as tight ion pairs whose binding is usually driven by cation/π interactions⁵⁶ between the portion of the *N*-alkyl pyridinium cation with the highest positive charge density and the π-rich aromatic cavity of the calix[4]arene host.^{25,55}

The NMR titrations were carried out in CDCl₃ solution using, for solubility reasons, only hosts **4b** and **4c**. In a typical titration experiment, progressive amounts of a 10⁻² M solution of the host were added to a 10⁻³ M solution of the pyridinium ion pair. In all titrations experiments the binding process was fast on the NMR timescale and the host addition induced a progressive up-field shift of the pyridinium ring resonances. The stack plot of Fig. 3 depicts some of the ¹H-NMR spectra collected during the titration of NMPI with **4c**. The large up-field shift endured by the pyridinium ring resonances upon addition of the host solution (*cf.* spectra *a* and *f* of Fig. 3) confirmed that the recognition of the ion-pair occurs between the NMP cation and the host aromatic cavities. More intriguing was the observation that the aromatic resonances of the NMP experience an up-field shift almost as twice as the one of the corresponding *N*-methyl resonance. The negligible shifts endured by the resonances of the hosts during the titrations were explained with a non significant conformational change of the calixarene scaffold upon guest binding. The down-field shift of ca. 0.15 ppm experienced by the calix[4]arene phenolic protons (*cf.* spectra *b* and *g* of Fig. 3) could be reasonably ascribed to such conformational changes rather than a real involvement of these groups in hydrogen bonding with the ion-pair counter anion

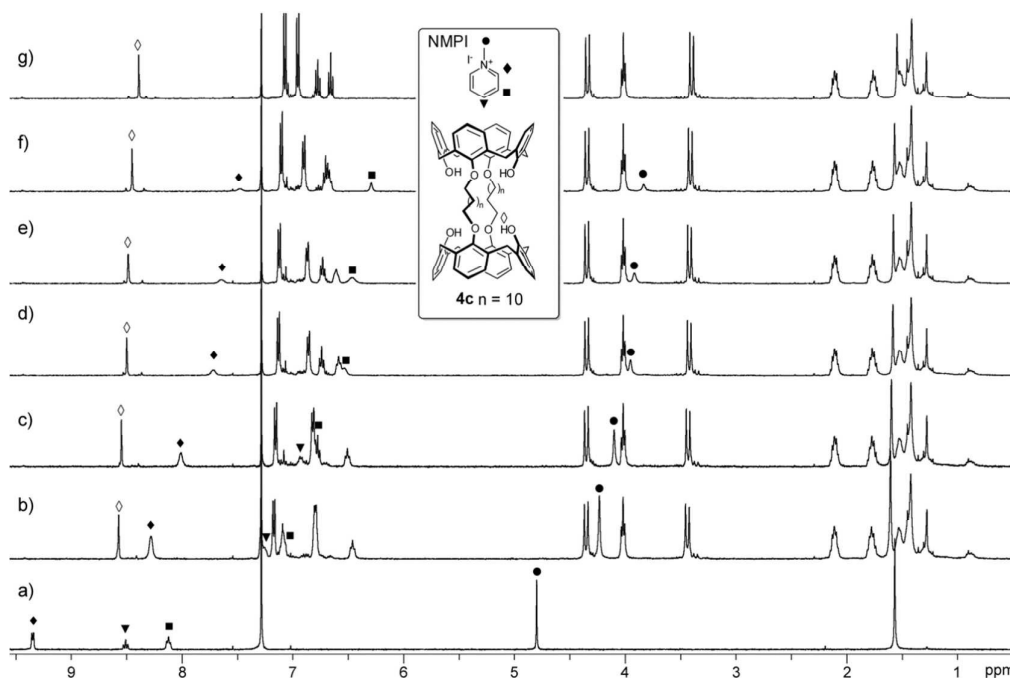


Fig. 3. ^1H -NMR stack plot (400 MHz, CDCl_3) for the titration of NMPI with **4c**: a) free NMPI; b) $[\text{NMPI}]/[\mathbf{4c}] = 2$; c) $[\text{NMPI}]/[\mathbf{4c}] = 1.6$; d) $[\text{NMPI}]/[\mathbf{4c}] = 1.1$; e) $[\text{NMPI}]/[\mathbf{4c}] = 0.9$; f) $[\text{NMPI}]/[\mathbf{4c}] = 0.5$; g) free **4c**. The resonances of the NMP cation were designed as follow: $\text{Py}^+\text{-Me}$ (●), $\text{Py}^+\text{-H ortho}$ (◆), $\text{Py}^+\text{-H meta}$ (■) and $\text{Py}^+\text{-H para}$ (▼); while the OHs resonances in the calix[4]arene semitube as (○).

Table 3. Apparent binding constants ($\log K_{1:1}$), theoretic chemical shift of the guest in the 100% complex formed (δ_∞) and observed up-field shift ($\Delta\delta_{\text{obs}}$, ppm) for the complexation of NMPX and NOPX ion pairs with monotopic (**5**) and ditopic (**4b-c**) calix[4]arenes.^{a,b}

Guest	$\log K_{1:1}^c$	δ_∞ (ppm) ^c	$\Delta\delta_{\text{obs}}$ (ppm) ^c	$\log K_{1:1}^d$	δ_∞ (ppm) ^d	$\Delta\delta_{\text{obs}}$ (ppm) ^d
NMPTsO	2.76(7)	3.62(6)	0.8	2.78(5)	6.8(1)	1.7
NMPBr	3.07(6)	3.79(4)	0.9	3.01(4)	7.19(6)	1.8
NMPI	3.08(3)	3.54(2)	1.0	3.04(2)	6.89(4)	2.0
NMPTf ₂ N	3.17(7)	3.73(4)	0.9	3.18(7)	7.19(7)	1.9
NMPBr + (6)	3.21(7)	3.37(4)	1.2	3.24(6)	6.89(7)	2.1
NOPBr	3.18(8)	4.39(2)	0.6	3.15(7)	7.40(8)	1.7
NOPI	3.13(4)	4.29(2)	0.6	3.17(4)	7.21(4)	1.8

^a Determined by ^1H NMR spectroscopic titrations at $T = 300$ K in CDCl_3 (standard deviations in parenthesis); initial concentration of the guest ion pair $c = 10^{-3}$ M, concentration of the titrant $c = 10^{-2}$ M; ^b $\Delta\delta_{\text{obs}} = \delta_{\text{free}} - \delta_{\text{guest}}$ where δ_{free} (ppm) is the chemical shift of the resonance of the free guest: NMPTsO, 9.24 (H_{ortho}) and 4.71 (N- CH_3); NMPBr, 9.43 (H_{ortho}) and 4.83 (N- CH_3); **6** + NMPBr, 9.23 (H_{ortho}) and 4.72 (N- CH_3); NMPI, 9.35 (H_{ortho}) and 4.77 (N- CH_3) ppm; NMPTf₂N, 9.41 (H_{ortho}) and 4.76 (N- CH_3); NOPBr, 9.39 (H_{ortho}) and 5.03 (N- CH_2 -) ppm; NOPI, 9.34 (H_{ortho}) and 5.00 (N- CH_2 -), while δ_{guest} is the chemical shift of the guest resonance at the end of the titration when the $[\mathbf{6}]/[\text{NMPX}]$ ratio is 3.57; ^c calculated by monitoring the chemical shift variation of the pyridinium ring *ortho* proton; ^d calculated by monitoring the chemical shift variation of the N- CH_3 (NMPX) or N- CH_2 - (NOPX).

The previous findings suggest a preferential binding mode in which the two almost parallel aromatic rings of the flattened π -rich cavity of the host envelope the electron poor pyridinium ring of the cation. This was indirectly confirmed by the evidence that also during the complexation of **4b** and **4c** with the series of the more sterically demanding NOPX ion-pairs, very similar results were found. For comparison, the series of NMPX and NOPX ion pairs was also titrated using the 1,3-dioctyloxy-calix[4]arene **5** (see Chart 1), which can be considered as the monotopic equivalent of the ditopic hosts **4b** and **4c**. This was accomplished to estimate the binding affinity for the *N*-alkyl pyridinium cation of a single aromatic cavity. In fact, differently from ditopic hosts **4b** and **4c**, host **5** can only

form 1:1 host-guest adducts and the non-linear fitting of the chemical shift variation experienced by the ion-pairs resonances can be easily carried out with the equation devised by Wilcox⁵⁷ to yield the apparent 1:1 binding constants $\log K_{1:1}$.[†] Among all the NMPX and NOPX resonances enduring an appreciable chemical shift variation upon addition of the host solution, the $\log K_{1:1}$ were calculated through the non-linear fitting of the shifts experienced by the resonance of the pyridinium *ortho* protons (Py-H ortho) as well as those of the *N*-methyl (NMPX, see Fig. 4) and N- CH_2 - (NOPX) protons.[‡]

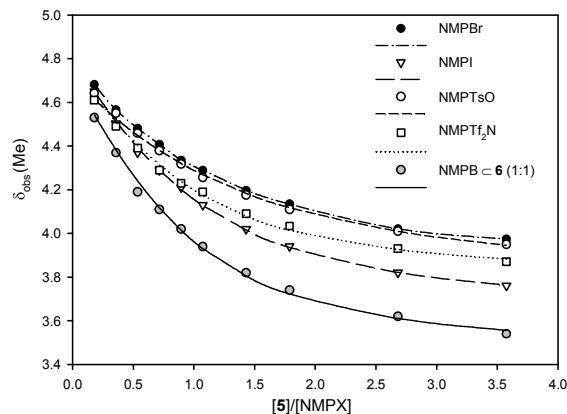
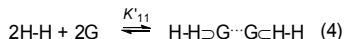
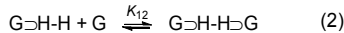


Fig. 4. Plots of the chemical shift variation endured by $N\text{-CH}_3$ NMR resonance of a series of NMPX ion pairs upon addition of host **5** in CDCl_3 solution at $T = 300\text{ K}$ (for the structure of the ion pairs and of the hosts see Chart 1).

Analysis of the results gathered in Table 3 evidences as, for each ion pair, the value of the $\log K_{1:1}$ is independent of the resonance used for their determination. Nevertheless, the observed up-field shift ($\Delta\delta_{\text{obs}}$) is generally higher for the Py-*H* *ortho* resonance rather than that of $N\text{-CH}_3$ and $N\text{-CH}_2$ protons (see Table 3 and Fig. 4). These findings seem to indicate an interaction between the ion pair and the calix[4]arene aromatic cavity with a preferential orientation of the pyridinium cation through its aromatic portion. This is probably due to steric hindrance induced by the anion which “sits” nearby the positively charged iminium nitrogen. A second and most important observation is that, as expected, the value of $\log K_{1:1}$ increases as the coordination strength of the anion does decrease (see e.g. 3.17 for NMPTf_2N vs. 2.76 for NMPTsO). Indeed, the highest value of $\log K_{1:1}$ was calculated for the titration of NMPBr in the presence of an equimolar amount of a tri-*n*-butylthioureido derivative of **6** (see Chart 1). This tris-urea-based compound,⁵⁸ is a host with a large affinity for spherical halide anions. Such “dual host approach” was previously used by us to favour the loosing of tight ion pair in weakly polar solvents.⁵⁹ The enwrapping of the anion by **6**, indeed, frees the NMP cation that can now more easily interact with the cavity of **5**. As a result the $\Delta\delta_{\text{obs}}$ determined for this titration experiment were the highest: 1.2 and 2.1 for the Py-*H* *ortho* and $N\text{-Me}$ resonances, respectively (see Table 3). Such behaviour was also evidenced by the comparison of the $N\text{-Me}$ resonance chemical shift variation in the series of NMPX ion pairs (see Fig. 4).

The Wilcox equation (see experimental) allows the calculation of binding constants from NMR titration data resulting from the formation of host/guest adducts with a 1:1 binding stoichiometry. Unfortunately, this powerful equation cannot handle the chemical shift variation deriving from multiple and concomitant equilibria such as those reasonably involving ditopic hosts **4b** and **4c** which were designed to interact simultaneously with two $N\text{-alkyl}$ pyridinium ion pairs thus giving rise to supramolecular adducts having 1:1 and 1:2 binding stoichiometry as shown by equilibria (1) and (2):⁶⁰



where H-H describes a generic ditopic host and G a generic guest. The overall binding process is described by equation (3).

To verify the correct stoichiometry of the binding process the method of continuous variation^{61,62} was applied in selected cases involving **4b** as the ditopic host and NMPI and NOPI as representative examples of $N\text{-alkylpyridinium}$ ion pairs. Two different experiments were devised (see experimental): by mixing in different ratios $5 \times 10^{-3}\text{ M}$ solutions of **4b** and NOPI, we obtained the smooth Job's plot denoted in fig. 5 by white circles. This plot reaches its maximum for molar fraction of the guest $X_{\text{NOPI}} \approx 0.6$ (see Fig. 5, white circles). When the reactants starting concentration was doubled (10^{-2} M) the Job's plot becomes sharper and its maximum shifted in correspondence of a guest molar fraction of $X_{\text{NOPI}} = 0.5$ (see Fig. 5, black circles).

These results suggest that at lower concentration, the equilibria described by equations (1) and (2) are coexistent in solution, while a 1:1 binding process is dominating when the NOPI concentration is increased. Similar results were found with NMPI. This totally unexpected result can be tentatively explained considering that this type of ion-pairs may give rise to large aggregates in weakly polar solvents, which represent the actual guest specie present in solution. It is thus reasonable to assume that when a host lacks of anion ancillary binding sites the complexation process may occur as described by equation (4), i.e. the ion pair is complexed as a dimer giving rise to an apparent 1:1 binding stoichiometry. On the other hand, the fast exchange conditions observed in the ^1H NMR titration experiments do not help to reveal the nature of this possible aggregation. Therefore, to verify the aggregation of the NMPI ion pairs, we devised a simple dilution experiment which was investigated by UV-vis spectroscopy. A series of absorption spectra of chloroform solution of NMPI at increasing concentration was collected in Fig. 6.

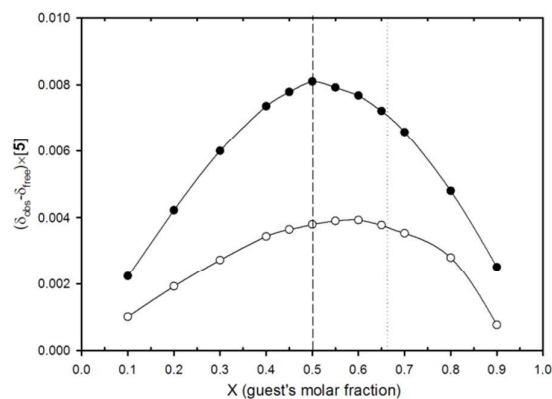


Fig. 5. Job's plots relative to the binding process between ditopic host **5** and NOPI. The experiments were carried out in CDCl_3 at $T = 300\text{ K}$ by mixing continuously (the total amount of moles in solution was kept constant) solutions of the interacting species of $5 \times 10^{-3}\text{ M}$ (○) and 10^{-2} M (●), respectively.

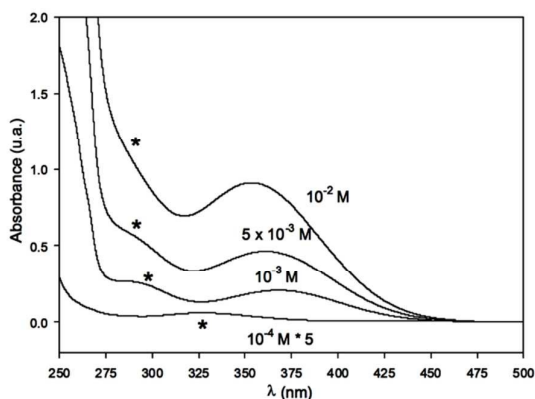


Fig. 6. UV-Vis spectra of solutions of NMPI in CHCl_3 at increasing concentration (the absorbance profile of the 10^{-4} M solution has been multiplied five times to evidence the band at 325 nm).

The spectrum of the 10^{-3} M solution (Fig. 6b) evidences two charge transfer (CT) bands centred at $\lambda = 370$ and 290 nm. Increasing the ion-pair concentration, the maximum position of both bands shifts to higher energy. At concentration of 10^{-2} M, the highest energy band (denoted with an asterisk in Fig. 6d) is barely recognised as a “shoulder” of an intense absorption due to the $\pi-\pi^*$ transition of the pyridine ring.⁶³ Contrariwise, both bands are red-shifted upon dilution to 10^{-4} M. Such shift at lower energy was explained as an ion-pair aggregation lessening. The results of the previous experiments indirectly confirmed that the stoichiometry of the binding between the ditopic hosts **4b-c** and the series of *N*-

alkylpyridium guests is strongly affected by aggregation of the ion pair to be bound. To reduce this undesired phenomenon, the binding experiments were carried out with more diluted solutions, using UV-vis spectroscopic titrations as the only reliable tool to calculate binding constants involving several concomitant equilibria in solution.⁶⁴

In a typical optical titration experiment, carried out in dichloromethane solution rather than in chloroform to improve the solubility of **4a**, increasing amounts of 10^{-3} M solutions of the hosts were added to 10^{-4} M solutions of the ion pairs (see experimental). UV-vis spectra of **4a-c** in CH_2Cl_2 are characterised by a strong absorption band centred at $\lambda \sim 285$ nm, which was never appreciably shifted upon complexation with either NMPX or NOPX ion pairs. UV-vis spectra of the NMPX and NOPX ion pairs sharing the same anion are identical. However, only the two bromides (NMPBr and NOPBr) and iodides (NMPI and NOPI) present in this solvent a non-hidden charge-transfer (CT) band exploitable for the titration experiments.⁶³ Indeed, upon addition of the host solution, such band usually underwent an intensity damping accompanied by a slight hypsochromic shift. As an example, the two collections of spectra recorded during the titration of NMPI and NMPBr with host **4b** have been gathered in Fig. 7. The blue-shift experienced by the CT bands of these salts, centred at $\lambda = 365$ and 320 nm for NMPI and NMPBr, respectively, is accompanied in both cases by the formation of an isosbestic point at $\lambda \approx 300$ nm (see Fig. 7).

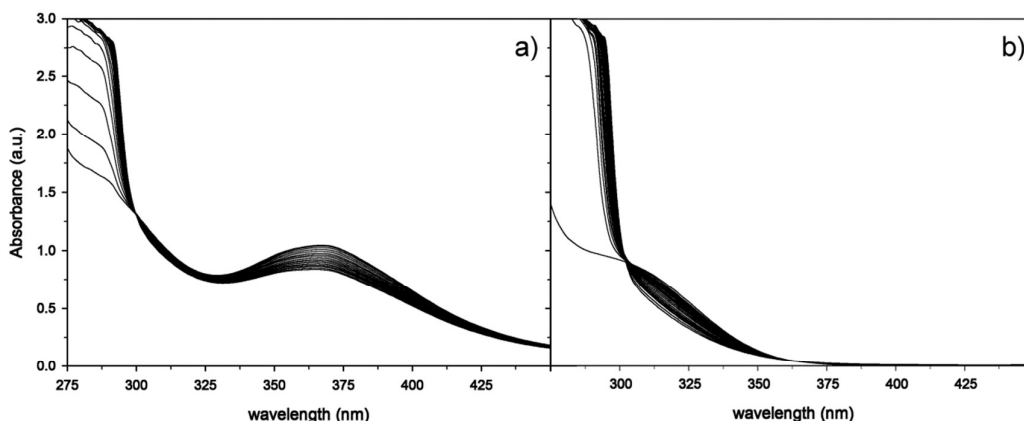


Fig. 7. Collection of UV-vis spectra (275 – 450 nm expansion) taken during the titrations in CH_2Cl_2 solution of a) NMPI and b) NMPBr with calix[4]arene semitube **4b**.

Another barely visible isosbestic point is found $\lambda \approx 365$ nm for NMPBr (see Fig. 7b) and at $\lambda = 460$ nm (not shown) for NMPI, evidencing that more than one binding equilibrium is present in solution. The shift of the CT band at higher energy can be explained considering that the interaction of the pyridinium cation with the host aromatic cavity contributes to a loosening of the ion pairing and a general stabilization of the more polar ground state of the charge transfer interaction generating this band.⁶⁵

The families of spectra collected during the titrations were fitted with the SpecFit/32 software.⁶⁶ In first instance, singular value decomposition (SVD) analysis was performed in order to estimate the number of species present in solution; then, a non-linear fitting of the optical data with the binding equilibria illustrated in equations (1) – (3) was used to calculate the binding constants. The results are gathered in Table 4 and it is worth to observe that a good fitting of the optical data was obtained only when the formation of 1:2 host-guest adducts was considered (equation 3). Among the series of ditopic hosts

4a-c, the highest values of $\log\beta$ were always calculated for **4b**, followed by **4c**. Except in the case of NMPBr binding by **4c**, the efficiency of these flexible hosts is significantly higher than the rigid **4a**. These results were explained considering that the rigidity of **4a** and the spatial proximity of its calix[4]arene subunits negatively affects the simultaneous binding of two positively charged NMP cations. This hypothesis was further supported by the observation that also the $\log\beta$ calculated for the longer and more flexible hosts **4b** and **4c** are never as twice as the value of the constants calculated for the corresponding monotopic host **5**. These results show that the formation of the 1:2 host – guest adduct is affected by a negative cooperative effect, i.e. the binding constant governing the equilibrium (2) is always smaller than the one governing equilibrium (1) ($\log K_{1:2} < \log K_{1:1}$). Finally, it is worth to mention that even using the bulkier *N*-octyl pyridinium salts (NOPBr and NOPI) as guests, the calculated binding constants are, within the experimental errors, very similar to those determined for the NMPX series (see Table 4).

Table 4. Overall binding constants ($\log\beta$ and $\log K_{1:1}$) for the complexation of NMPX and NOPX (with X = Br and I) ion pairs in CH₂Cl₂ solution with ditopic (**4a-c**) and monotopic (**5**) calix[4]arene hosts.^a

Host	NMPBr	NMPI	NOPBr	NOPI
4a	6.2(7)	5.0(1)	5.0(1)	6.4(7)
4b	8.1(3)	8.4(2)	7.7(1)	8.2(2)
4c	6.8(1)	8.4(2)	7.2(1)	7.4(2)
5	4.3(1)	4.2(2)	3.5(7)	4.1(1)

^a Determined at room temperature through UV-vis spectrophotometric titrations.

Conclusions

In summary, we have synthesised three head-to-head calix[4]arene semitubes (**4a-c**) characterised by two linking alkyl chains of different length. The X-rays crystal structures of two of these homoditopic receptors show different binding properties towards one of the two solvent used for their crystallization. The crystal structure of **4b**, in which the two calix[4]arene subunits are connected through two hexyl chains, evidences the potential of these new ditopic hosts for the construction supramolecular polymers. The binding properties of these hosts have been evaluated in solution in weakly polar media toward a series of pyridinium ion pairs. NMR and UV-vis spectroscopy measurements show that hosts are able to recognise simultaneously two guest ion-pairs. Studies to insert on these hosts ancillary binding sites for the simultaneous recognition of both the cation and its counter anion as guests are undergoing in our laboratories.

Experimental

General

All reactions were carried out under nitrogen; all solvents were freshly distilled under nitrogen and stored over molecular sieves for at least 3h prior to use. NMR spectra were recorded

on Bruker Avance instruments operating at 300 and 400 MHz for ¹H and 100 MHz for ¹³C. Chemical shift reported are referred to residual solvent resonances. ESI-MS spectra were recorded with Infusion Waters Acquity Ultra Performance LC instrument. UV-Visible spectra were recorded with a Lambda Bio 20 instrument. Melting points are uncorrected, and were recorded with Electrothermal instrument. Silica gel layers (SiO₂, MERCK 60 F254) were used for thin layer chromatography (TLC). 60 Å silica gel (MERCK, 0.04-0.063 mm, 230-240 mesh) were used for column chromatography. NMPX and NOPX salts,²⁵ compounds **2a**,⁶⁷ **2b**,⁶⁸ **3**,⁶⁹ **5**,⁷⁰ **6**⁵⁸ were synthesised according to reported procedures. All other reagents were of reagent grade quality as obtained from commercial suppliers and were used without further purification.

Synthetic procedures

General procedure for the synthesis of calix[4]arene semitubes 4a-c. A solution of calix[4]arene **3** (3 g, 0.007 mol) and K₂CO₃ (2 g, 0.014 mol) in CH₃CN (150 mL) was refluxed under vigorous stirring for 10 minutes. After this period, the appropriate ditosylate **2a-c** (0.014 mol) was added. The resulting mixture was refluxed for further 3 days, cooled to room temperature and evaporated to dryness under reduced pressure. The residue was taken up with 50 mL of a 10% v/v solution of HCl and CH₂Cl₂ (200 mL). The separated organic phase was washed thrice with water (3×25ml), dried over anhydrous Na₂SO₄, and evaporated to dryness under reduced pressure.

Calix[4]arene semitube 4a: purification of the solid residue by trituration with chloroform afforded **4a** in 60% yield as a white solid compound. m.p.>300 °C; ¹H NMR (CD₂Cl₂, 300 MHz) δ (ppm): 8.90 (s, 4H, -OH); 7.11 (d, 8H, *J* = 7.5 Hz, ArH); 7.09 (d, 8H, *J* = 7.4 Hz, ArH); 6.89 (t, 4H, *J* = 7.5 Hz, ArH); 6.65 (t, 4H, *J* = 7.4 Hz, ArH); 4.46 (d, 8H, *J* = 12.8 Hz, Ar-CH₂-Ar axial); 4.39 (t, 8H, *J* = 8 Hz, OCH₂CH₂-); 3.51 (d, 8H, *J* = 12.8 Hz, Ar-CH₂-Ar equatorial); 3.16 (q, 4H, *J* = 8 Hz, OCH₂CH₂CH₂); ¹³C NMR (CD₂Cl₂, 100 MHz): δ (ppm) 153.6; 151.9; 134.9; 129.6; 129.0; 129.0; 126.1; 120.0; 73.0; 32.2; 31.2; ESI-MS (*m/z*) = 951 [M+Na]⁺; elemental analysis for C₆₂H₅₆O₈, calcd.: C 80.17, H 6.03; obs.: C 80.35, H 6.28.

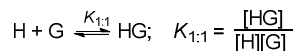
Calix[4]arene semitube 4b: purification of the solid residue by column chromatography (eluent: CH₂Cl₂/hexane = 6/4) afforded **4b** in 30% yield as a white solid compound. m.p.> 300 °C; ¹H NMR (CDCl₃, 300 MHz): δ (ppm) 8.45 (s, 4H, -OH); 6.99 (d, 8H, *J* = 7.5 Hz, ArH); 6.91 (d, 8H, *J* = 7.5 Hz, ArH); 6.74 (t, 4H, *J* = 7.5 Hz, ArH); 6.62 (t, 4H, *J* = 7.4 Hz, ArH); 4.23 (d, 8H, *J* = 12.9 Hz, Ar-CH₂-Ar axial); 4.03 (t, 8H, *J* = 6.7 Hz, OCH₂(CH₂)₄-); 3.21 (d, 8H, *J* = 12.9 Hz, Ar-CH₂-Ar equatorial); 2.9-2.8 (m, 8H, OCH₂CH₂(CH₂)₂-); 2.0-1.9 (m, 8H, OCH₂CH₂(CH₂)₂-); ¹³C NMR (CDCl₃, 100 MHz): δ (ppm) 153.3; 151.7; 133.6; 128.8; 128.4; 128.0; 125.3; 118.8; 75.9; 31.2; 30.1; 24.9; ESI-MS (*m/z*) = 1035 [M+Na]⁺; *m/z* = 1052 [M+K]⁺; elemental analysis for C₆₈H₆₈O₈: calc. C 80.60, H 6.76; obs. C 80.91, H 7.13.

Calix[4]arene semitube 4c: purification of the solid residue by column chromatography (eluent: hexane/ethyl acetate = 7/3) afforded **4c** in 10% yield as a white solid compound. m.p. > 300 °C; $^1\text{H NMR}$ (CDCl_3 , 300 MHz): δ (ppm) 8.41 (s, 4H, -OH); 7.07 (d, 8H, $J = 7.5$ Hz, ArH); 6.96 (d, 8H, $J = 7.5$ Hz, ArH); 6.78 (t, 4H, $J = 7.5$ Hz, ArH); 6.67 (t, 4H, $J = 7.5$ Hz, ArH); 4.34 (d, 8H, $J = 12.9$ Hz, Ar-CH₂-Ar axial); 4.07 (t, 8H, $J = 6.3$ Hz, OCH₂(CH₂)₁₁-); 3.40 (d, 8H, $J = 12.9$ Hz, Ar-CH₂-Ar equatorial); 2.2–2.0 (m, 8H, OCH₂CH₂(CH₂)₈-); 1.8–1.7 (m, 8H, OCH₂CH₂CH₂(CH₂)₆-); 1.6–1.2 (4m, 24H, OCH₂CH₂CH₂(CH₂)₆-); $^{13}\text{C NMR}$ (CDCl_3 , 100 MHz): δ (ppm) 153.3; 151.7; 133.6; 128.8; 128.4; 128.0; 125.3; 118.8; 75.9; 31.2; 30.6 (2 res.); 30.3 (2 res.); 25.0; ESI-MS (m/z) = 1204 $[\text{M}+\text{Na}]^+$; m/z = 1220 $[\text{M}+\text{K}]^+$; elemental analysis for $\text{C}_{80}\text{H}_{92}\text{O}_8$: calc. C 81.32, H 7.85; obs. C 81.01, H 7.97.

Binding Studies

$^1\text{H-NMR}$ continuous variation methods (Job's plot). Aliquots of stock solutions in CDCl_3 of the calix[4]arene host and of the corresponding *N*-alkyl pyridinium organic salt were added to several 5-mm NMR tubes in different ratios maintaining the total molar concentration constant. In this way, 12–14 samples in which the mole fraction (x) of the interacting species was continuously varied from 0.1 to 1 were prepared. A $^1\text{H NMR}$ spectrum was recorded for each sample. The corresponding Job plot was obtained plotting a property proportional to the complex concentration, in this case $(\delta_{\text{obs}} - \delta_{\text{free}}) \times [\text{guest}]_0$, versus the mole fraction of the salt. δ_{obs} and δ_{free} represent the chemical shift (ppm) of a resonance of the pyridinium cation in the complex and in the free salt, respectively. The stoichiometry of binding is obtained from the value of the mole fraction in abscissa that yields the maximum of the plot. For $x = 0.5$, the stoichiometry of binding is 1; for $x = 0.66$ the stoichiometry of binding is H:G = 1:2

$^1\text{H-NMR}$ titrations. Solutions (500 μl) in CDCl_3 of the organic salt (usually $c = 10^{-3}$ M) were prepared in a 5 mm NMR tube and small aliquots of a tenfold concentrated solution of the calix[4]arene host (usually $c = 10^{-2}$ M) in CDCl_3 were added. A $^1\text{H NMR}$ spectrum was recorded after each addition. Considering a 1:1 host-guest binding equilibrium, the apparent binding constant is expressed by the following equation:



where $[\text{H}]$, $[\text{G}]$, and $[\text{HG}]$ are the concentrations of the calix[4]arene receptor, of the organic salt and of the complex at the equilibrium, respectively. The binding constants K were calculated through the non-linear fitting of the chemical shift variation of the protons of the organic salt using the equation devised by Wilcox:⁵⁷

$$\delta_{\text{obs}} = \delta_{\text{free}} + \frac{\Delta\delta_{\text{sc}}}{2[\text{G}]_0} \left[\frac{1}{K_{1:1}} + [\text{H}]_0 + [\text{G}]_0 - \sqrt{\left(\frac{1}{K_{1:1}} + [\text{H}]_0 + [\text{G}]_0 \right)^2 - 4[\text{H}]_0[\text{G}]_0} \right]$$

$$\Delta\delta_{\text{sc}} = \delta_{\text{sc}} - \delta_{\text{free}}$$

where δ_{obs} , δ_{free} , δ_{sc} , $[\text{H}]_0$, and $[\text{G}]_0$ are the observed chemical shift of the proton under investigation in fast exchange condition, the chemical shift of same proton in the non-bound "free" salt and in the complex (guessed), the initial concentration of the guest and of the host for each titration point, respectively. The conditions of the Weber parameter p ($[\text{conc. of the complex}]/[\text{maximum possible conc. of the complex}]$) were verified for each titration experiment according to the calculated binding constant.⁵⁷ If necessary the concentrations of the two reactants were adjusted and the NMR titration experiment repeated to explore the proper p range (0.2–0.8).

UV-vis titrations. Optical spectroscopic titrations were carried out in a quartz cuvette (path length = 1 cm), maintained at 300 K through an external thermostat, by adding small aliquots of a dichloromethane solution ($c = 1 \times 10^{-4}$ M) of the calix[4]arene host to a dichloromethane solution ($c = 2 \times 10^{-5}$ M) of the NMPX or NOPX ($X = \text{Br}, \text{I}$) ion pair. The spectral data were collected in the 265–900 nm wavelength range. The binding constants were calculated selecting different binding models with the Specfit/32 software.⁶⁶ The fitting of the spectral data was carried out considering the optical variation in the sampled wavelength range. As for the NMR titrations, the Weber parameter p was checked against the calculated binding constant.

Table 5. Crystal data and experimental details for data collection and structure refinement for **4a** and **4b**.

Compound	4a	4b
Empirical formula	C ₆₂ H ₅₆ O ₈ •CH ₂ Cl ₂	C ₆₈ H ₆₈ O ₈ •2CHCl ₃
Formula weight	1098.985	1252.036
Crystal size [mm]	0.2x0.3x0.3	0.3x0.4x0.3
Crystal system	Triclinic	Triclinic
Space group	<i>P</i> -1	<i>P</i> -1
<i>a</i> [Å]	10574(1)	15.114(1)
<i>b</i> [Å]	15.785(1)	19.254(1)
<i>c</i> [Å]	17.417(1)	12.036(1)
α [°]	88.866(2)	103.11(1)
β [°]	89.179(2)	104.06(1)
γ [°]	75.592(2)	102.42(1)
<i>V</i> [Å ³]	2815.0(5)	3170.8(5)
<i>Z</i>	2	2
ρ (calcd.) [g/cm ³]	1.297	1.311
<i>F</i> (000)	1152	1312
<i>T</i> [K]	298	298
λ [Å]	.71069	1.54178
μ [mm ⁻¹]	0.266	2.915
Index ranges	-13 ≤ <i>h</i> ≤ 13 -20 ≤ <i>k</i> ≤ 20 -22 ≤ <i>l</i> ≤ 22	-18 ≤ <i>h</i> ≤ 8 -18 ≤ <i>k</i> ≤ 23 -14 ≤ <i>l</i> ≤ 14
Refl. collected	36740	12648
Independent refl.	12371 (<i>R</i> _{int} = 0.045)	11963 (<i>R</i> _{int} = 0.154)
Obs. reflections	6573 <i>F</i> _o ≥ 4 σ (<i>F</i> _o)	6108 <i>F</i> _o ≥ 4 σ (<i>F</i> _o)
parameters	689	762
<i>R</i> ₁	0.0998	0.109
<i>wR</i> ₂	0.341	0.35
Goodness-of-fit on ^[a]	1.112	1.119

^[a] $R_1 = \sum ||F_o| - |F_c|| / \sum |F_o|$, $wR_2 = [\sum w(F_o^2 - F_c^2)^2 / \sum w F_o^4]^{1/2}$. Goodness-of-fit = $[\sum w(F_o^2 - F_c^2)^2 / (n-p)]^{1/2}$, where *n* is the number of reflections and *p* the number of parameters.

Crystallography. Crystallographic data for **4a** and **4b** were collected on a Siemens AED diffractometer using graphite monochromatic CuK α radiation and were summarised in Table 5. The intensities were corrected for Lorentz, polarization and absorption effects. The structures were solved by direct methods using SIR2004⁷¹ and refined on *F*² by full-matrix least-squares methods, using SHELXL-97.⁷² All the non-hydrogen atoms were refined with anisotropic atomic displacements. For **4b** the structure contains two CHCl₃ solvent molecules for each calix[4]arene semitube sub-unit. All the non-hydrogen atoms were refined with anisotropic atomic displacements. The hydrogen atoms were included in the last cycles of the refinement at idealised geometry (C-H and O-H 0.96 Å) and refined in the “riding” model with isotropic atomic displacements 1.2 times their U_{eq} their parent atoms. Geometric calculations were performed with the PARST97.⁷³

Acknowledgements

The authors thank the Centro Interdipartimentale di Misura of the University of Parma for NMR and MS measurements. This work was supported by the Italian MIUR (2010CX2TLM) and by the University of Parma.

Notes and references

¥ The lack of complexing properties in the solid state for ditopic hosts **4b** and **4c** failures was tentatively explained considering that the high flexibility of their bridging alkyl spacers should not favour the formation of ordered units in the crystal lattice. For the intrinsically more rigid host **4a**, its poor solubility even in dichloromethane, is reasonably the main cause of such failures (see also NMR binding studies).

† The binding constants ($\log K_{1:1}$) are considered as apparent because in the equation used for their calculations the reactants' concentration is inserted in place of the more correct “activity”.

‡ The up-field shift of these resonances was never hidden by the resonances of the host throughout the titrations.

§ In a previous work it has been shown that a cationic complex between NMP and a monotopic calix[4]arene host self-assemble in the solid state giving rise to clusters of six calixarene-NMPI units in a columnar arrangement. In this structure the iodide anions are interdigitated between the cationic complexes along the same crystallographic axis (see Ref. 25).

§§ An apparent 1:1 binding stoichiometry could be also the result of higher isodesmic stoichiometry of binding, such as: 2:2, 3:3 and so on.

- G. M. Whitesides and B. A. Grzybowski, *Science*, 2002, **295**, 2418–2421.
- G. M. Whitesides and M. Boncheva, *Proc. Natl. Acad. Sci.*, 2002, **99**, 4769–4774.
- J. W. Steed, D. R. Turner and K. Wallace, *Core Concepts in Supramolecular Chemistry and Nanochemistry*, John Wiley & Sons, Ltd, Chichester (UK), 2007.
- A. Ciferri, Ed., *Supramolecular Polymers*, CRC Press, Boca Raton, 2005.
- A. Harada, Ed., *Supramolecular Polymer Chemistry*, Wiley-VCH Verlag GmbH & Co. KGaA, Weinheim, Germany, 2011.
- T. F. A. De Greef, M. M. J. Smulders, M. Wolffs, A. P. H. J. Schenning, R. P. Sijbesma and E. W. Meijer, *Chem. Rev.*, 2009, **109**, 5687–5754.
- L. Brunsveld, B. J. B. Folmer, E. W. Meijer and R. P. Sijbesma, *Chem. Rev.*, 2001, **101**, 4071–4098.
- C. Fouquey, J.-M. Lehn and A.-M. Levelut, *Adv. Mater.*, 1990, **2**, 254–257.
- R. J. Wojtecki, M. A. Meador and S. J. Rowan, *Nat. Mater.*, 2011, **10**, 14–27.
- Z. Zhang, Y. Luo, J. Chen, S. Dong, Y. Yu, Z. Ma and F. Huang, *Angew. Chem. Int. Ed.*, 2011, **50**, 1397–1401.
- A. Harada, Y. Takashima and H. Yamaguchi, *Chem. Soc. Rev.*, 2009, **38**, 875–882.
- B. Zheng, F. Wang, S. Dong and F. Huang, *Chem. Soc. Rev.*, 2012, **41**, 1621–1636.
- S. Dong, B. Zheng, F. Wang and F. Huang, *Acc. Chem. Res.*, 2014, **47**, 1982–1994.
- C. D. Gutsche, *Calixarenes: An Introduction*, Royal Society of Chemistry, Cambridge, 2nd edn., 2008.
- D. Garozzo, G. Gattuso, F. H. Kohnke, A. Notti, S. Pappalardo, M. F. Parisi, I. Pisagatti, A. J. P. White and D. J. Williams, *Org. Lett.*, 2003, **5**, 4025–4028.
- S. Pappalardo, V. Villari, S. Slovak, Y. Cohen, G. Gattuso, A.

- Notti, A. Pappalardo, I. Pisagatti and M. F. Parisi, *Chem. Eur. J.*, 2007, **13**, 8164–8173.
- 17 G. Gattuso, A. Notti, A. Pappalardo, M. F. Parisi, I. Pisagatti, S. Pappalardo, D. Garozzo, A. Messina, Y. Cohen and S. Slovak, *J. Org. Chem.*, 2008, **73**, 7280–7289.
- 18 D.-S. Guo and Y. Liu, *Chem. Soc. Rev.*, 2012, **41**, 5907–5921.
- 19 V. Villari, G. Gattuso, A. Notti, A. Pappalardo and N. Micali, *J. Phys. Chem. B*, 2012, **116**, 5537–5541.
- 20 E. Dalcanale and R. Pinalli, Calixarenes-Based Supramolecular Polymers in *Encyclopedia of Polymeric Nanomaterials*, eds. S. Kobayashi and K. Müllen, Springer Berlin Heidelberg, Berlin, Heidelberg, 2014.
- 21 J. H. Lee, J. Park, J.-W. Park, H.-J. Ahn, J. Jaworski and J. H. Jung, *Nat. Commun.*, 2015, **6**, 6650.
- 22 F. Rodler, B. Schade, C. M. Jäger, S. Backes, F. Hampel, C. Böttcher, T. Clark and A. Hirsch, *J. Am. Chem. Soc.*, 2015, **137**, 3308–3317.
- 20 R. K. Castellano, D. M. Rudkevich and J. Rebek, *Proc. Natl. Acad. Sci.*, 1997, **94**, 7132–7137.
- 23 L. Pescatori, A. Arduini, A. Pochini, A. Secchi, C. Massera and F. Ugozzoli, *CrystEngComm*, 2009, **11**, 239–241.
- 24 F. Ciesia, A. Plech, C. Mattioli, L. Pescatori, A. Arduini, A. Pochini, F. Rossi and A. Secchi, *J. Phys. Chem. C*, 2010, **114**, 13601–13607.
- 25 L. Pescatori, A. Arduini, A. Pochini, A. Secchi, C. Massera and F. Ugozzoli, *Org. Biomol. Chem.*, 2009, **7**, 3698–3708.
- 26 P. M. S. Monk, *The Viologens*, John Wiley & Sons, Ltd, Chichester (UK), 1998.
- 27 A. Credi, S. Dumas, S. Silvi, M. Venturi, A. Arduini, A. Pochini and A. Secchi, *J. Org. Chem.*, 2004, **69**, 5881–5887.
- 28 D.-S. Guo, H.-Y. Zhang, C.-J. Li and Y. Liu, *Chem. Commun.*, 2006, **1**, 2592–2594.
- 29 C. Gaeta, T. Caruso, M. Mincoelli, F. Troisi, E. Vasca and P. Neri, *Tetrahedron*, 2008, **64**, 5370–5378.
- 30 L. Erra, C. Tedesco, G. Vaughan, M. Brunelli, F. Troisi, C. Gaeta and P. Neri, *CrystEngComm*, 2010, **12**, 3463–3466.
- 31 X. Su, D.-S. Guo and Y. Liu, *CrystEngComm*, 2010, **12**, 947–952.
- 32 R. K. Castellano and J. Rebek, *J. Am. Chem. Soc.*, 1998, **120**, 3657–3663.
- 33 T. F. A. de Greef and E. W. Meijer, *Nature*, 2008, **453**, 171–173.
- 34 D.-S. Guo, S. Chen, H. Qian, H.-Q. Zhang and Y. Liu, *Chem. Commun.*, 2010, **46**, 2620–2622.
- 35 X. Ma, R. Sun, W. Li and H. Tian, *Polym. Chem.*, 2011, **2**, 1068–1070.
- 36 X. Ma and H. Tian, *Acc. Chem. Res.*, 2014, **47**, 1971–1981.
- 37 X. Yang, H. Yu, L. Wang, R. Tong, M. Akram, Y. Chen and X. Zhai, *Soft Matter*, 2015, **11**, 1242–1252.
- 38 C. Bonaccorso, A. Ciadamidaro, C. Sgarlata, D. Sciotto and G. Arena, *Chem. Commun.*, 2010, **46**, 7139–7141.
- 39 C. Bonaccorso, C. Sgarlata, G. Grasso, V. Zito, D. Sciotto and G. Arena, *Chem. Commun.*, 2011, **47**, 6117–6119.
- 40 H. X. Zhao, D. S. Guo and Y. Liu, *J. Phys. Chem. B*, 2013, **117**, 1978–1987.
- 41 P. R. A. Webber, P. D. Beer, G. Z. Chen, V. Felix and M. G. B. Drew, *J. Am. Chem. Soc.*, 2003, **125**, 5774–5785.
- 42 P. Webber and P. D. Beer, *Dalton Trans.*, 2003, 2249–2252.
- 43 T. Nabeshima, T. Saiki, K. Sumitomo and S. Akine, *Tetrahedron Lett.*, 2004, **45**, 4719–4722.
- 44 N. Kerdpaiboon, B. Tomapatanaget, O. Chailapakul and T. Tuntulani, *J. Org. Chem.*, 2005, **70**, 4797–4804.
- 45 P. R. A. Webber, A. Cowley, M. G. B. Drew and P. D. Beer, *Chem. Eur. J.*, 2003, **9**, 2439–2446.
- 46 S. E. Matthews, P. Schmitt, V. Felix, M. G. B. Drew and P. D. Beer, *J. Am. Chem. Soc.*, 2002, **124**, 1341–1353.
- 47 E. Pinkhassik, V. Sidorov and I. Stibor, *J. Org. Chem.*, 1998, **63**, 9644–9651.
- 48 A. Arduini, G. Giorgi, A. Pochini, A. Secchi and F. Ugozzoli, *Tetrahedron*, 2001, **57**, 2411–2417.
- 49 A. Arduini, E. Brindani, G. Giorgi, A. Pochini and A. Secchi, *Tetrahedron*, 2003, **59**, 7587–7594.
- 50 G. Arena, A. Contino, E. Longo, G. Spoto, A. Arduini, A. Pochini, A. Secchi, C. Massera and F. Ugozzoli, *New J. Chem.*, 2004, **28**, 56–61.
- 51 O. Takahashi, Y. Kohno and M. Nishio, *Chem. Rev.*, 2010, **110**, 6049–6076.
- 52 M. Nishio, *Phys. Chem. Chem. Phys.*, 2011, **13**, 13873–13900.
- 53 S. Tsuzuki, K. Honda, T. Uchimaru, M. Mikami and K. Tanabe, *J. Phys. Chem. A*, 2002, **106**, 4423–4428.
- 54 S. Tsuzuki, K. Honda, T. Uchimaru, M. Mikami and A. Fujii, *J. Phys. Chem. A*, 2006, **110**, 10163–10168.
- 55 A. Arduini, A. Pochini and A. Secchi, *Eur. J. Org. Chem.*, 2000, **2000**, 2325–2334.
- 56 J. C. Ma and D. A. Dougherty, *Chem. Rev.*, 1997, **97**, 1303–1324.
- 57 C. S. Wilcox, in *Frontiers in Supramolecular Organic Chemistry and Photochemistry*, eds. H. J. Schneider and H. Durr, VCH, 1991, pp. 123–144.
- 58 K. Jeong, K. Hahn and Y. L. Cho, *Tetrahedron Lett.*, 1998, **39**, 3779–3782.
- 59 A. Arduini, E. Brindani, G. Giorgi, A. Pochini and A. Secchi, *J. Org. Chem.*, 2002, **67**, 6188–6194.
- 60 K. A. Connors, *Comprehensive Supramolecular Chemistry*, Pergamon, Oxford, 1996.
- 61 C. Y. Huang, *Enzyme Kinetics and Mechanism - Part C: Intermediates, Stereochemistry, and Rate Studies*, Elsevier, 1982, vol. 87.
- 62 Z. D. Hill and P. MacCarthy, *J. Chem. Educ.*, 1986, **63**, 162–167.
- 63 J. S. Brinen, J. G. Koren, H. D. Olmstead and R. C. Hirt, *J.*

ARTICLE

Journal Name

- Phys. Chem.*, 1965, **69**, 3791–3794.
- 64 P. Thordarson, *Chem. Soc. Rev.*, 2011, **40**, 1305–1323.
- 65 E. M. Kosower, *J. Am. Chem. Soc.*, 1958, **80**, 3253–3260.
- 66 R. A. Binstead, *SPECFIT*; Spectrum Software Associates: Chapel Hill, NC, 1996.
- 67 M. Nakamura, H. Yokono, K. Tomita, M. Ouchi, M. Miki and R. Dohno, *J. Org. Chem.*, 2002, **67**, 3533–3536.
- 68 V. Pejanović, V. Piperski, D. Ugljesić-Kilibarda, J. Tasić, M. Dacević, L. Medić-Mijacević, E. Gunić, M. Popsavin and V. Popsavin, *Eur. J. Med. Chem.*, 2006, **41**, 503–512.
- 69 A. Arduini and A. Casnati, in *Macrocyclic Synthesis: A Practical Approach*, ed. D. Parker, Oxford University Press, Oxford, 1996, pp. 145–172.
- 70 A. Arduini, M. Fabbi, M. Mantovani, L. Mirone, A. Pochini, A. Secchi and R. Ungaro, *J. Org. Chem.*, 1995, **60**, 1454–1457.
- 71 M. C. Burla, R. Caliandro, M. Camalli, B. Carrozzini, G. L. Cascarano, L. De Caro, C. Giacovazzo, G. Polidori and R. Spagna, *J. Appl. Crystallogr.*, 2005, **38**, 381–388.
- 72 G. M. Sheldrick, *SHELX97*; Program for Crystal Structure Refinement, Göttingen (GER), 1997.
- 73 M. Nardelli, *J. Appl. Crystallogr.*, 1996, **29**, 296–300.